frontiers | Frontiers in Earth Science

TYPE Original Research
PUBLISHED 09 September 2024
DOI 10.3389/feart.2024.1473904

OPEN ACCESS

EDITED BY
Haijun Qiu,
Northwest University, China

REVIEWED BY
Linjuan Xu,
Yellow River Institute of Hydraulic Research, China
Na He,
Henan Polytechnic University, China

*CORRESPONDENCE
Jiakun Wang,
13508131369@163.com

RECEIVED 31 July 2024
ACCEPTED 27 August 2024
PUBLISHED 09 September 2024

CITATION
Ren J, Wang J, Chen R, Li H, Xu D, Yan L and Song J (2024) Remote sensing identification of shallow landslide based on improved otsu algorithm and multi feature threshold. *Front. Earth Sci.* 12:1473904. doi: 10.3389/feart.2024.1473904

Remote sensing identification of shallow landslide based on improved otsu algorithm and multi feature threshold

Jing Ren, Jiakun Wang*, Rui Chen, Hong Li, Dongli Xu, Lihua Yan and Jingyuan Song

Sichuan Leshan Geological Engineering Survey Institute Group Co., Ltd, Leshan, Sichuan, China

In low-resolution remote sensing images under complex lighting conditions, there is a similarity in spectral characteristics between non-landslide areas and landslide bodies, which increases the probability of misjudgment in the identification process of shallow landslide bodies. In order to further improve the accuracy of landslide identification, a shallow landslide remote sensing identification method based on an improved Otsu algorithm and multi-feature threshold is proposed for the temporary treatment project of the Yangjunba disaster site in Leshan City. Using Retinex theory, remote sensing images are enhanced with local linear models and guided filtering; then, multi-feature scales and sliding window calculations of opening and closing transformations identify potential landslide areas, which are finally segmented using the Otsu algorithm. Through experimental verification, the method proposed in this article can clearly segment the target object and background after binary segmentation of remote sensing images. The recognition rate of shallow landslide bodies is not less than 95%, indicating that the method proposed in this article is relatively accurate in identifying shallow landslide bodies in the research area and has good application effects.

KEYWORDS

otsu algorithm, multi feature threshold, remote sensing images, landslide mass, image segmentation

1 Introduction

Global climate change has led to a significant increase in the number and scale of rainfall landslides, posing greater threats to human activity areas such as roads, houses, farmland, and residential areas (Amarasinghe et al., 2024). The initial stage of a rainfall landslide is a shallow landslide that occurs on the surface or in shallow soil (Su et al., 2024). Therefore, how to effectively identify and monitor shallow landslide bodies has become an important issue that urgently needs to be addressed in the field of geological disaster prevention and control (Wang et al., 2024). Remote sensing technology has demonstrated unique advantages in identifying and monitoring geological hazards (Liang and Sun, 2023). Through the interpretation of remote sensing images, rapid identification and dynamic monitoring of landslide bodies can be achieved, involving the accuracy of landslide disaster identification and monitoring efficiency and providing strong technical support for geological disaster prevention and control.

In the face of increasingly severe environmental changes and geological disasters, it is particularly important to study remote sensing identification methods for shallow landslide bodies.

Jiang W et al. (2023) proposed a landslide disaster remote sensing image recognition method based on AED Net (Attention combined with Encoder De der Network). Optimizing the multi-scale feature extraction capability of deep neural networks using shallow feature extraction networks and combining the feature restoration ability of the encoder-decoder structure to restore the boundary information of landslide disaster remote sensing images, an AED Net model is constructed to complete landslide disaster identification. This method does not consider the close spectral characteristics between non-landslide areas and landslide bodies, significantly increasing the probability of misjudgment in identifying landslide bodies under background interference.

Du et al. (2023) proposed a high-resolution remote sensing image landslide identification and detection method based on DETR. Using the Transformer as the primary research method and combining the advantages of convolutional neural networks, a DETR network was constructed to augment the remote sensing images dataset through offline data augmentation algorithms. By leveraging the structural advantages of the encoder-decoder, the DETR network was trained and predicted to identify landslide changes in remote sensing images (Liu et al., 2024). However, when the landslide mass is small, or the remote sensing image resolution is low, DETR may have difficulty accurately segmenting the shallow landslide mass from the background, resulting in poor detection performance.

Xin et al. (2023) proposed combining image recognition technology with computer vision technology to extract local deformation features of landslides and monitor the entire slope. At the same time, time series image data was combined with machine vision data for analysis, and a landslide model was used to simulate the deformation and displacement during the landslide process. The deformation and displacement of the landslide were verified by combining drone orthophoto data (Qiu et al., 2024). However, landslide monitoring often faces complex and variable environmental conditions, such as changes in lighting, weather influences (such as rain, fog, snow, etc.), and vegetation coverage. These factors may lead to a decrease in image quality, thereby affecting the accuracy of recognition and monitoring.

Zheng et al. (2024) used LiDAR data to extract geomorphic features and analyzed the deformation characteristics of landslide locations using InSAR technology. The deformation rate and range were determined through time-series deformation information, and the landslide boundary was identified using unmanned aerial vehicle radar (Wei et al., 2024). The principle of geometric distortion was used to correct remote sensing images, achieving real-time monitoring of landslide deformation. However, in complex lighting environments, using only geometric distortion correction as a method is difficult to effectively enhance the clarity of remote sensing images, which affects the subsequent recognition of shallow landslide targets that are difficult to detect.

In response to the problem that existing research methods are difficult to accurately identify small shallow landslide bodies in low-resolution remote sensing images under complex lighting environments, this paper proposes a shallow landslide body remote sensing identification method based on the improved Otsu algorithm and multi-feature threshold 1 (He et al., 2024a). Innovatively combining Retinex enhancement and guided filtering methods to enhance the clarity of remote sensing images in complex lighting scenarios. Due to the complex terrain information contained in remote sensing images, in order to segment small shallow landslide targets in complex backgrounds and distinguish various spectral features between non-landslide areas and landslide bodies, this paper uses multiple feature thresholds to remove invalid or redundant background features, thereby improving the accuracy of image segmentation. The traditional Otsu algorithm can perform image segmentation by automatically selecting a threshold in image processing. However, it is easy to ignore the spatial relationship of pixels and reduce the segmentation effect. Therefore, this paper innovatively uses the Monte Carlo iteration strategy to improve it, optimize the flexibility and applicability of landslide remote sensing identification, and improve the accuracy and efficiency of identification.

2 Data and method

2.1 Data

2.1.1 Overview data of the experimental area

This article takes the temporary remediation project of the Yangjunba disaster site in Suji Town, Yanlong Village, Shizhong District, Leshan City, as the research object and conducts remote sensing identification research on shallow landslide bodies. The geographical coordinates of this area are E: 103°39′0.49″, N: 29°34′20.81″, and the elevation range of the exploration area is roughly between 400 and 500 m. The geomorphic features are hills with significant undulations and steep slopes in some areas. There are also rural roads leading directly to the landslide area, providing convenient transportation conditions. The landslide body is located in an “m” - shaped micro gully area on a hill slope, with a rear edge elevation of 455 m and a front edge elevation of 407 m, with a height difference of 48 m. The landslide body is tongue-shaped and has a regular shape. It extends from the north side to the exposed bedrock, from the south side to the deformation boundary of the landslide, from the east side (front edge of the landslide) to the houses and village roads of the villagers, and from the west side (rear edge of the landslide) to the exposed bedrock. The landslide mass in this area has been deformed since July 2018, with transverse tensile cracks appearing in the middle of the slope and signs of forward movement of the retaining walls of some houses at the front edge. On 6 August 2019, Leshan was hit by an extremely heavy rainstorm once in 50 years, with a maximum daily rainfall of 380 mm. After the heavy rainfall, the landslide mass in this area was deformed again, and a downward dislocation crack appeared at the rear edge. The deformation of the retaining wall behind the house was aggravated, and the soil mass of the steep slope collapsed. In August 2020, the central district of Leshan City experienced another general rainstorm, with continuous rainfall from the 15th to the 17th, and the maximum rainfall intensity from 11:00 on the 17th to 2:00 on the 18th, exceeding 50 mm/h, leading to the aggravation of mountain deformation. At present, the landslide is about 110 m long and 55 m wide along the slope, with an area of about 6,050 square meters. The main sliding direction of the landslide is 115°, and there

FIGURE 1
Local landslide cracks.

are tensile cracks of varying widths at the rear and middle of the landslide. Among them, the deformation of the central tensile crack is the most significant, with a width of about 30–40 cm, a north-south direction, and an extension length of about 27 m. On the right boundary, there is a sunken crack deformation with a width of about 5–15 cm, running nearly east-west and extending for about 110 m. On the right side of the retaining wall behind Xie Renzhong's house at the front edge of the landslide, perennial clear water can be seen flowing out between the bedrock layers, while on the back edge of the landslide, brick red sandstone bedrock is exposed, with a rock attitude of 310°∠ 4°. The middle crack L1 and the north crack L2 of the landslide in this area are shown in Figure 1.

The landslide stability is poor, and large-scale collapse and damage are possible. Therefore, it is necessary to conduct remote sensing image recognition of shallow landslide bodies in this area to identify the geological hazard characteristics of the landslide, which is representative of the experimental target.

2.1.2 Experimental remote sensing data

In response to the on-site landslide case, five wide-swath panchromatic remote sensing images were captured using the Gaofen-1 satellite, and landslide recognition experiments were conducted based on the image data. The remote sensing image of the research area is shown in Figure 2.

The width size of these images is 8,192×2048 pixels, with a pixel width of 8 bits, and the data volume of a single image reaches 128 Mbit. In order to improve recognition accuracy, images with significant differences in grayscale values were selected, where the ground area contains interference factors such as vegetation with higher grayscale values. Divide satellite image data and digital elevation model data based on spectral characteristics and spatial resolution. The digital elevation model of the region is shown in Figure 3, and the data parameter information is shown in Table 1.

2.2 Method

Figure 4 shows the shallow landslide remote sensing identification process based on the improved Otsu algorithm and multi-feature threshold studied in this article.

According to the process shown in Figure 4, firstly, the remote sensing image is enhanced and smoothed based on the Retinex theory and the local linear model. Then, multi-scale feature values of the remote sensing image background and landslide targets are extracted. Finally, the Otsu algorithm is used to segment the remote-sensing images of landslide bodies. Improve the binary threshold processing of the Otsu algorithm, use the optimal threshold to segment the image into foreground and background, and achieve remote sensing recognition of shallow landslide bodies.

2.2.1 Image preprocessing replace

Remote sensing images may be affected by various factors, such as atmospheric disturbances, cloud cover, sensor noise, etc., during transmission and acquisition (Tao et al., 2022). Therefore, the accuracy of recognition can be improved by enhancing remote-sensing images (Lin et al., 2023). However, using a single enhancement method alone may not achieve the desired effect (Ye et al., 2024). Therefore, this article innovatively combines the Retinex enhancement and guided filtering methods to adapt to this complex lighting scene, improving the processing effect and practicality of remote sensing images.

The Retinex theory emphasizes color constancy, which means that the color perception on the surface of an object should remain consistent under changing lighting conditions (Yang et al., 2024). It can effectively handle highlight and shadow areas in the image, making the brightness distribution of the image more uniform and also restoring color information lost due to lighting changes in the image (Li et al., 2023). Guided filtering uses a guided image

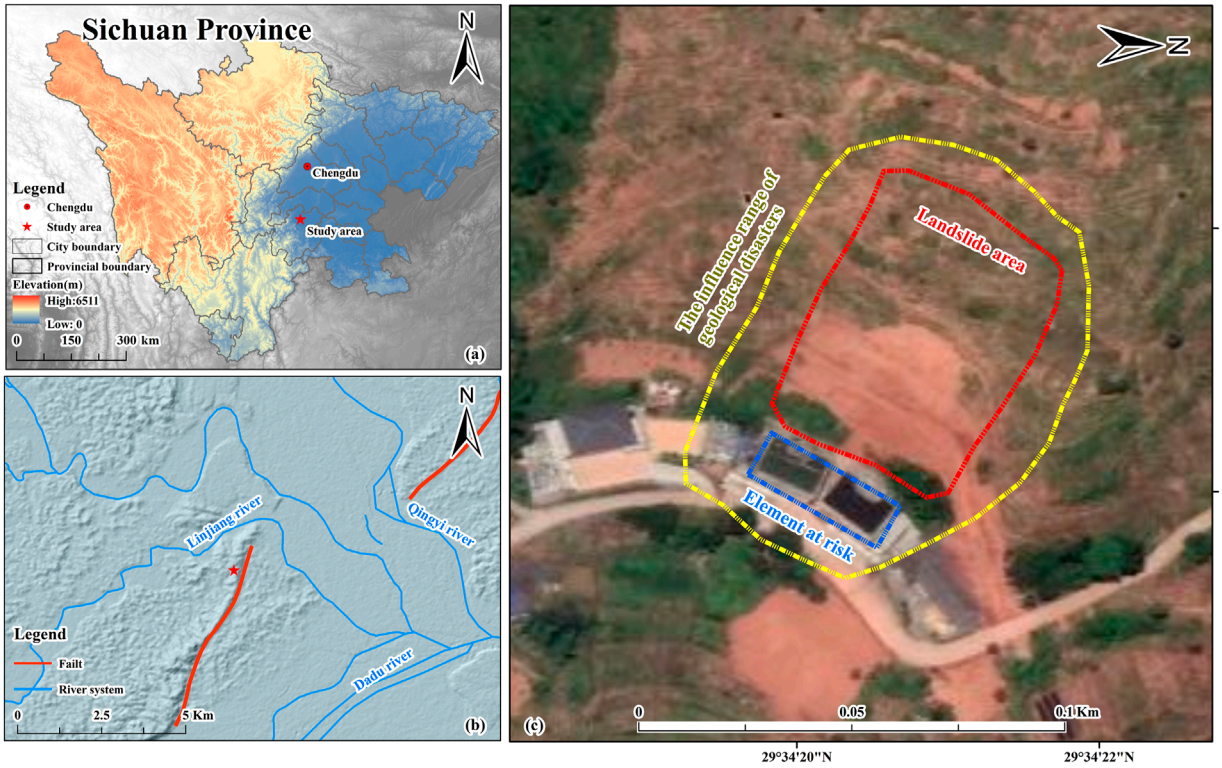

FIGURE 2
Location of the study area and the general situation of the landslide.

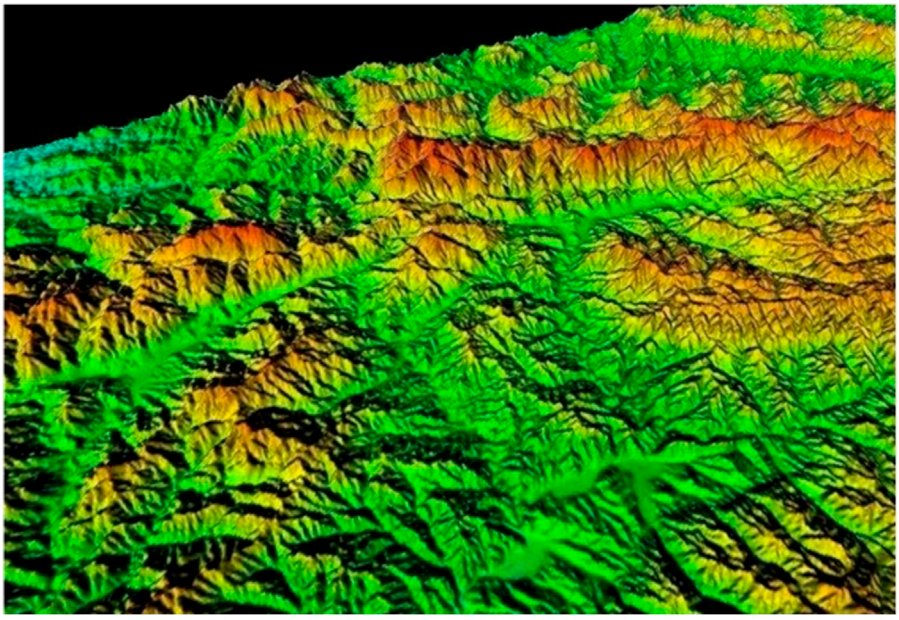

FIGURE 3
DEM model.

TABLE 1 Raw data parameter information.

Raw data	Spectral range/μm	Spatial resolution/m
Gaofen-1 (GF-1) Satellite imagery data	0.45~0.90	2.00
	0.45~0.52	8.00
	0.52~0.59	
	0.63~0.69	
	0.77~0.89	
Digital Elevation Model (DEM)	—	30.00

Input the DEM, model and remote sensing data of working conditions into the Revit2020 database. Divide the database data into training and testing sets in a 3:1 ratio. The training set data is input into the TensorFlow model training and learning framework for training processing, while the test set data is used for testing.

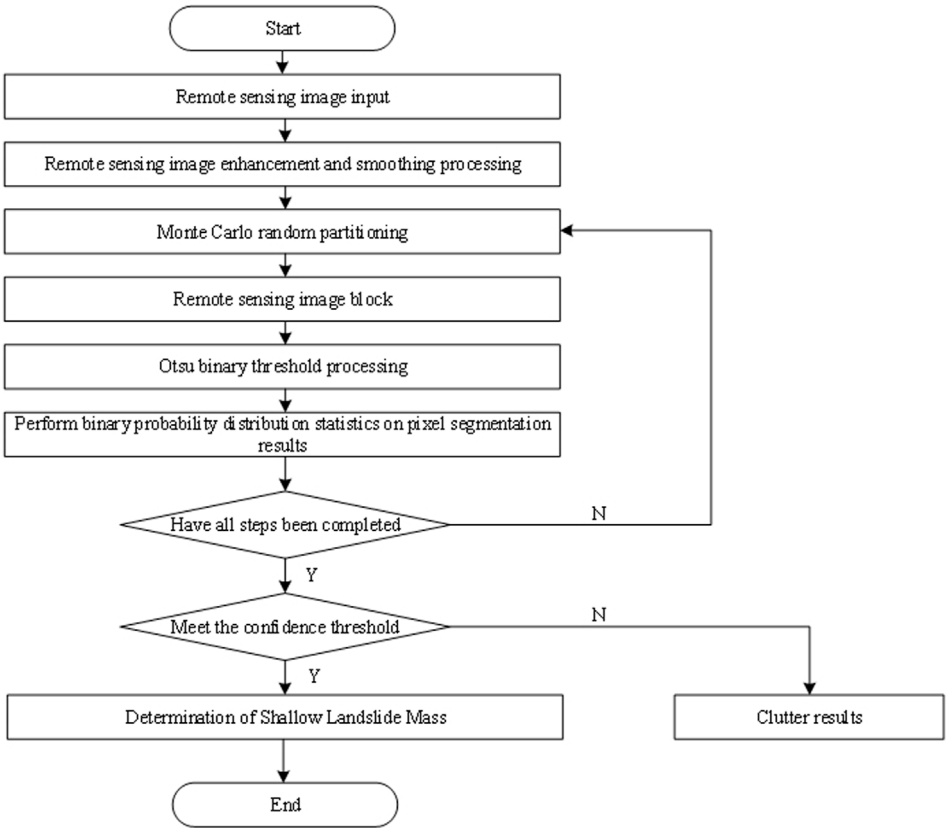

FIGURE 4
Remote sensing image segmentation and recognition process.

to guide the filtering process. Compared to other edge-preserving filtering methods, such as bilateral filtering, guided filtering has lower computational complexity. It can process large-scale images faster, making it suitable for preprocessing high-resolution remote-sensing images. However, it has disadvantages in color enhancement of low-resolution images. The Retinex enhancement performs well in dynamic range compression, edge enhancement, and color restoration but may have shortcomings in smoothing processing. Guided filtering is adept at achieving smoothing while preserving edge information (Panigrahi and Gupta, 2022). The combination of the two can compensate for their respective shortcomings and achieve a more comprehensive image enhancement effect by starting from image enhancement and image smoothing (He et al., 2024b). Therefore, this article combines the Retinex enhancement algorithm and guided filtering algorithm to preprocess remote sensing images.

2.2.1.1 Remote sensing image enhancement processing based on retinex

The Retinex enhancement method can effectively handle the quality loss caused by uneven lighting on shallow landslide remote sensing images, improve the brightness, contrast, and color expression of the images, and enhance the clarity of remote sensing images. In the Retinex algorithm, shallow landslide remote sensing images can be represented as:

$$S(i,j) = L(i,j) \times R(i,j) \tag{1}$$

In the formula, $S(i,j)$ represents the original shallow landslide remote sensing image; (i,j) represents the pixel points of shallow landslide remote sensing images; $L(i,j)$ and $R(i,j)$ represent the illumination component and reflection component, respectively.

The irradiation component mainly involves light source conditions, including factors such as solar position, angle, and atmospheric conditions. These factors can affect the brightness distribution and contrast of ground objects in remote sensing images, thereby affecting the identification and analysis of landslide bodies. The reflection component is related to the physical properties and geometric shape of surface objects, including the material, humidity, roughness, etc., of landslide bodies (He et al., 2023). These factors will affect the reflection characteristics of the landslide body to light, and to some extent, affect the characteristics of the landslide body in remote sensing images. Multi-Scale Retinex (MSR) can adjust the contrast and brightness of an image while preserving its detailed information. In order to highlight the characteristics of the landslide body and improve the readability of the image, it is necessary to process the illumination $L(i,j)$ by removing or reducing the influence of the illumination component, thereby highlighting the reflection component that reflects the surface characteristics of the object. The calculation formula for MSR is:

$$\lg R(i,j) = \lg S(i,j) - \lg [G * L(i,j)] \tag{2}$$

In the formula, $*$ is the convolution operation; G stands for Gaussian filter scale, and its calculation formula is:

$$G = u \exp\left[\frac{-(i^2 - j^2)}{\sigma^2}\right] \tag{3}$$

In the formula, u represents Gaussian filter; σ stands for Gaussian kernel.

After filtering through multiple Gaussian kernels, the reflection components at this scale can be extracted to enhance the color and detail of shallow landslide remote sensing images and obtain Retinex-enhanced remote sensing images $I(i,j)$. The calculation formula is:

$$I(i,j) = \sum_{m=1}^{N} W_m \{\lg S(i,j) - \lg R(i,j) + g[G * S(i,j)]\} \tag{4}$$

In the formula, W_m represents the fusion weight in the m-th number field.

After completing color detail enhancement, the edges of low-resolution remote sensing images in complex lighting scenes are prone to blurring, so smooth filtering is required.

2.2.1.2 Smooth processing of remote sensing images based on guided filtering

To further enhance the edge details of shallow landslide remote sensing images, a local linear model guided by filtering is used to apply smoothing filtering to the obtained enhanced remote sensing image $I(i,j)$, improving the edge details of the image. The calculation formula is:

$$q_i = a_h C_i + b_h, \quad \forall i \in h \tag{5}$$

In the formula, q_i represents the output image of the guided filtering algorithm after filtering pixel i in remote sensing image $I(i,j)$; a_h and b_h represent the linear coefficients of remote sensing images during filtering processing; h represents the window used in the smoothing filtering process; C_i represents the radius of the window for pixel i during the smoothing filtering process. Using q_i as the guiding image, substitute remote sensing image $I(i,j)$ and apply the minimum cost function to constrain its implementation. The calculation formula is:

$$E(q_i) = \sum_{i \in h} \left[(a_h C_i + b_h - p_i)^2 + \varepsilon a_h^2\right] \tag{6}$$

In the formula, p_i represents the number of pixels; ε stands for regularization parameter.

Using linear regression analysis method, the remote sensing images under guided filtering are smoothed to obtain the smoothed shallow landslide remote sensing image $J(i,j)$. The calculation formula is:

$$J(i,j) = \frac{1}{\sigma_h^2 + \varepsilon} \frac{1}{|h| E(q_i)} \sum_{i \in h} C_i p_i - u p_h \tag{7}$$

In the formula, u represents the number of iterations of the local linear model smoothing filtering process; p_h stands for pixel mean.

Based on Formulas 1–7, complete remote sensing image preprocessing using the Retinex enhancement algorithm and guided filtering algorithm, providing clear image data for subsequent landslide identification.

2.2.2 Landslide feature extraction replace

Remote sensing images typically contain complex terrain information, such as water bodies, vegetation, buildings, etc., which exhibit different features in the image, such as color, texture, shape, etc. Multi-feature thresholds can be used to screen for features that have a significant impact on the segmentation results of the target, removing invalid or redundant features (Deng et al., 2024; Senogles et al., 2023). By setting reasonable threshold conditions, the most representative subset of landslide target features can be selected to more finely distinguish between these terrain backgrounds and landslide targets, thereby improving the accuracy of image segmentation.

In the task of landslide segmentation and recognition, traditional recognition models often rely on the spectral information features of a single pixel target to classify and determine landslide bodies. However, current hyperspectral remote sensing images reveal that even within potential landslide areas, differences in spectral information between different regions may be significant, while spectral features between certain non-landslide areas and landslide bodies may be closer (Niu et al., 2023; Peters et al., 2024). This phenomenon greatly increases the noise interference

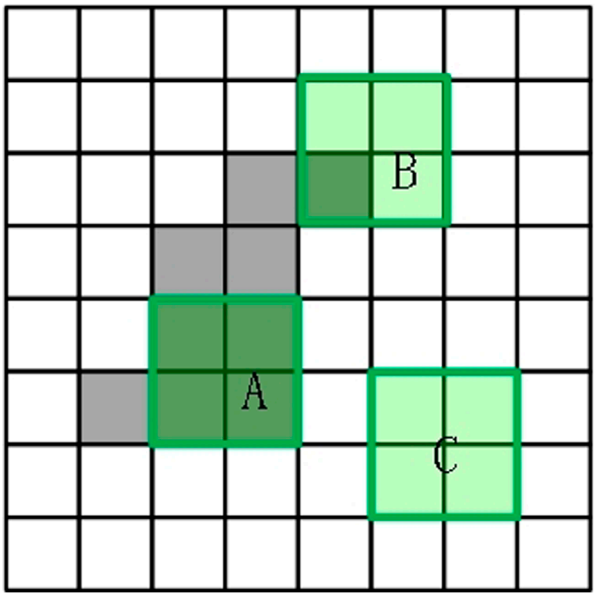

FIGURE 5
The process of extracting morphological features from remote sensing images.

in the landslide identification process, which can easily lead to misjudgment, such as misclassifying non-landslide areas as landslide bodies or omitting landslide bodies. Therefore, this article delves into and integrates multiple spectral features in remote-sensing images based on traditional single-pixel spectral features. These features can capture subtle spatial changes in the landslide body and its surrounding environment, such as abnormal changes in surface morphology, specific patterns of vegetation coverage, etc., providing richer information for accurate identification of landslide bodies. By comprehensively utilizing these features, it is possible to better depict the spatial details of landslide bodies and improve the accuracy and reliability of landslide body identification. Therefore, in the process of multi-feature extraction for landslide identification, special attention is paid to the extraction of spatial features, which contain geographical information about the landslide and its surrounding environment and are crucial for accurate identification of the landslide. Spatial features can be further subdivided into morphological features and attribute features (Rajan et al., 2024).

In the extraction of morphological features, a fixed-sized window is used to slide scan remote sensing images. By operating this switch window, the connected pixel regions in the remote sensing image are identified and connected, which often reflect key spatial features such as the shape contour and edge changes of the landslide body, effectively highlighting the spatial distribution characteristics of the landslide body. The entire extraction process can be visually demonstrated through a diagram, as shown in Figure 5:

In Figure 5, the green box represents the ABC window range, and the gray block refers to the target area. The white block is the background area. The annotated sliding window is considered a key structural unit for landslide identification, where A, B, and C represent three typical situations that the window may encounter when scanning landslide remote sensing images. Window A simulates an idealized scenario where the feature values (such as spectral reflectance, texture features, etc.) of all pixels within the window are almost equal. This is rare in actual landslide recognition and may indicate uniform regions or specific backgrounds in the image. Window B reflects a more common situation in landslide identification, where at least one pixel in the area covered by the window has a feature value that is not equal to other points. This difference may be caused by changes in geological features at the edge of the landslide body, different parts of the landslide body, or differences in vegetation coverage, which are crucial for identifying the morphology, scale, and boundaries of the landslide body. Window C describes an extreme situation where all expected pixel feature values within the window are significantly different from those outside the window boundary. This situation may indicate a strong contrast between the landslide body and the surrounding environment, such as the contrast between the exposed rocks of the landslide body and the dense vegetation around it, which is of great significance for quickly locating the location of the landslide body. However, in practical applications, the situation of window C is relatively rare and requires careful handling to avoid misjudgment. The transformation function for opening and closing the above window is as follows:

$$\begin{cases} s(f_1(J(i,j))) = (f \odot s) \oplus s \\ s(f_0(J(i,j))) = (f \oplus s) \odot s \end{cases} \tag{8}$$

In the formula, $s(f)_1$ represents the transformation function under the window opening operation; $s(f)_0$ represents the transformation function under window closure operation; s stands for sliding window; f represents the area covered by the window; The $\oplus$ symbol represents the characteristic changes of expansion; $\odot$ represents the characteristic changes of corrosion.

After extracting morphological features using the above formula, it is also necessary to extract attribute features from remote-sensing images for landslide recognition. Extract feature vectors of length 2n from each pixel for images of different resolutions. By using dimensionality reduction techniques, these high-dimensional data are effectively compressed while preserving key information and arranging feature values in an orderly manner to reflect their importance. The core of the attribute feature extraction process for landslide identification lies in the use of carefully designed attribute filters, which calculate the feature values of the potential coverage area of the landslide based on specific attribute sets such as terrain slope, vegetation index, soil moisture, etc. (Kusunose et al., 2022). During this process, the selection and definition of attributes are highly flexible and can be customized according to the specific characteristics and recognition needs of the landslide mass. For a given detection area and threshold conditions, due to the complexity and diversity of landslide bodies, direct feature mapping in low-dimensional space often fails to fully reflect their characteristics. Therefore, this article extends the low dimensional spatial attribute features in the high-dimensional feature space to capture more subtle information that is helpful for landslide identification:

$$E = T\{A_1(P_1), A_2(P_2), ..., A_n(P_m)\} \tag{9}$$

In the formula, E represents the attribute characteristic values of the potential coverage area of the landslide mass; T stands

for attribute set; $A_1 \sim A_n$ represents feature value ranking; $P_1 \sim P_m$ represents attribute feature categories, such as terrain slope, vegetation index, soil moisture, etc.

Formulas 8, 9 can be used to extract features from landslide remote-sensing images based on multiple feature thresholds. The extracted features can be used to segment the background and identify landslide targets.

2.2.3 Landslide segmentation replace

In the field of image processing and remote sensing recognition, the Otsu algorithm is widely used for its ability to automatically select the optimal threshold for image segmentation, which can effectively distinguish landslide bodies (i.e., target foreground) from the surrounding environment (i.e., background) (Neogi et al., 2024). Therefore, after completing the feature extraction of landslide remote sensing images based on multiple feature thresholds, the Otsu algorithm was selected to segment the landslide remote sensing images. However, the traditional Otsu algorithm needs to traverse all possible gray levels and calculate their corresponding inter-class variances when searching for the optimal threshold. This process requires a huge amount of computation when processing high-resolution or large data images, resulting in low algorithm efficiency and difficulty meeting real-time requirements. To overcome this limitation, this article innovatively uses the Monte Carlo iterative method to optimize the remote sensing identification effect of landslide bodies. As the sample size increases, the results of the Monte Carlo method will become closer to the true solution, with high flexibility and applicability.

Firstly, by applying the Otsu algorithm, the pixels in the local image are divided into two categories: one represents the high brightness or specific grayscale value range of the landslide body, and the other represents the low brightness or different grayscale value range of the background (König et al., 2022; Zhu et al., 2024). Assuming that the shallow landslide remote sensing image $J(i,j)$ processed by smoothing enhancement in section 2.1 can be divided into $\{0,1,\cdots,F\}$ gray levels, where the total number of pixels corresponding to gray level F is F_b and its proportion is $B_b = F_b / \sum_{b=0}^{F} F_b$, then $\sum_{b=0}^{F} B_b = 1$. Using grayscale value d as the threshold for segmenting landslide mass and background in remote sensing images, the pixels in interval $[0,d]$ can be regarded as background D_0, and the pixels in interval $[d,F]$ can be regarded as landslide mass target D_1. Then, the proportion η_0 of background pixels and the average grayscale value μ_0 in the remote sensing image are calculated as follows (Equation 10):

$$\begin{cases} \eta_0 = \sum_{b=0}^{d} B_b s(f_1(J(i,j))) \\ \mu_0 = \frac{1}{\eta_0} \sum_{b=0}^{d} B_b s(f_0(J(i,j))) \end{cases} \tag{10}$$

The proportion η_1 and gray value mean μ_1 of landslide target pixels in landslide remote sensing images are as follows (Equation 11):

$$\begin{cases} \eta_1 = \sum_{b=d}^{d} B_b E \\ \mu_1 = \frac{1}{\eta_1} \sum_{b=d}^{d} B_b E \end{cases} \tag{11}$$

The calculation formula for the average grayscale value μ of landslide remote sensing images is as follows (Equation 12):

$$\mu = \eta_0 \mu_0 + \eta_1 \mu_1 \tag{12}$$

Then, the Monte Carlo iterative strategy is used to optimize the remote sensing image of the landslide body. Firstly, the large remote sensing image is segmented into multiple smaller local image regions using random partitioning techniques (Jiang et al., 2023). This process aims to reduce the computational complexity of directly processing the entire image and allow for a more refined analysis of each local region. Evaluate the confidence level of the binarization effect within each block based on the random samples generated by the Monte Carlo iteration process and their processing results. The calculation of confidence can be based on factors such as the stable appearance of feature patterns in multiple iterations, the consistency of classification results, and the degree of conformity with other known information. High-confidence segmentation means that the landslide identification results are more reliable, while low-confidence segmentation may require further analysis or validation (Shen et al., 2023). Based on the above block processing and binary recognition results, combined with the fusion technology of panchromatic images and terrain data, the accuracy and comprehensiveness of landslide identification can be further improved. Full-color images provide rich texture and detail information, which helps to more accurately depict the morphology and boundaries of landslide bodies. Terrain data (such as DEM) provides key information about surface morphology, slope changes, etc., which are crucial for understanding the causes, development trends, and potential risks of landslide bodies. The specific operational approach is as follows:

(1) Based on the ratio of the number of morphological features $s(f_1(J(i,j)))$ and attribute features E extracted from the remote sensing image in Section 2.2, the size of the Monte Carlo random block of the remote sensing image is set to $H \times W$, and the Monte Carlo calculation steps are N steps. Monte Carlo random block is performed according to this setting.

(2) Using Monte Carlo to perform Otsu binary thresholding on remote sensing images. Determine the optimal threshold d through inter class variance, so that the image can be divided into foreground (target object, i.e., landslide) and background parts based on this threshold. The inter class variance θ^2 between D_0 and D_1 can be obtained as follows (Equation 13):

$$\theta^2 = \mu(D_0 - D_1) = \eta_0(\mu_0 - \mu)^2 + \eta_1(\mu_1 - \mu)^2 = \eta_0\eta_1(\mu_0 - \mu_1)^2 \tag{13}$$

The inter class variance θ^2 can be used to determine the optimal threshold of the Otsu algorithm. When the θ^2 takes its maximum value, the difference between D_0 and D_1 is the largest, and the corresponding gray value threshold d of the landslide remote sensing image is the optimal threshold.

(3) Monte Carlo iteration itself is based on random sampling and does not directly correspond to a mathematical formula. But the sampling process can be based on a random number generation algorithm to calculate the binary probability distribution $P(i,j)$ as follows (Equation 14):

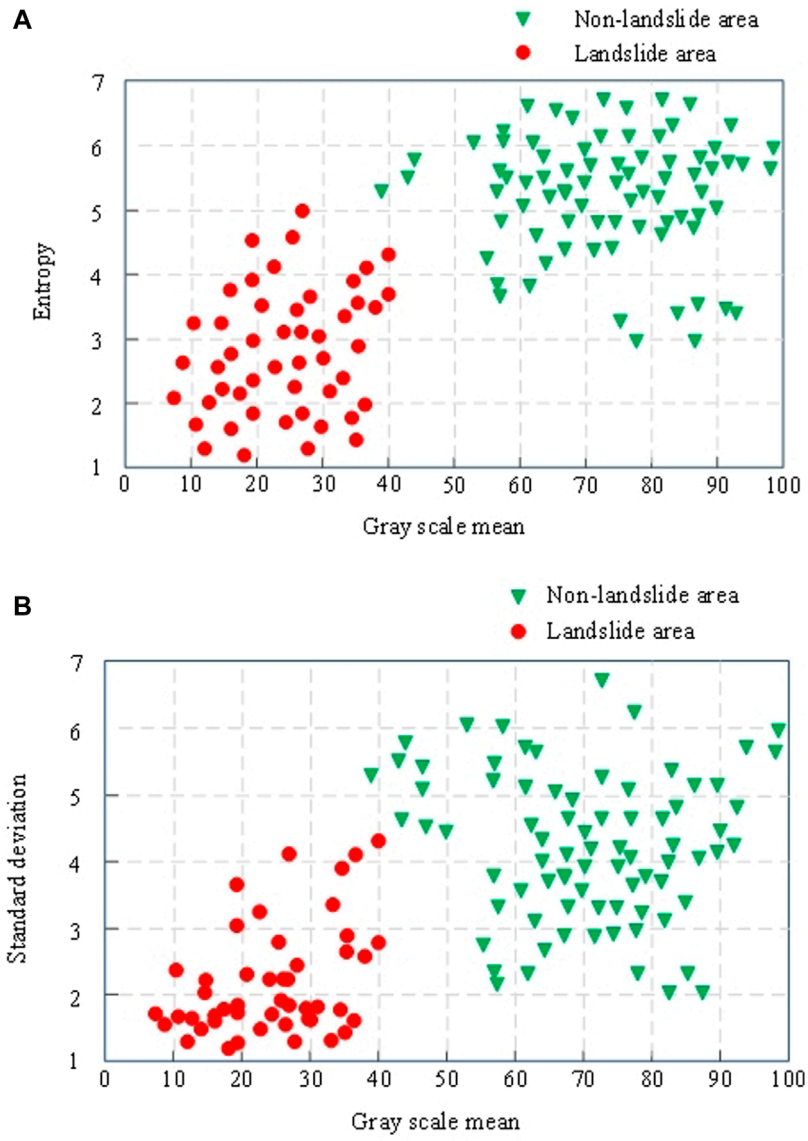

FIGURE 6
(A) Comparison of local window entropy and grayscale mean **(B)** Comparison of local window standard deviation and grayscale mean.

$$P(i,j) = \frac{1}{N}\sum_{k=1}^{N} \theta^2 O_k(i,j) \tag{14}$$

In the formula, O_k represents obtaining the binary segmentation result for each pixel, where $k \in N$.

(4) Set the confidence level T_P as the probability threshold, with a value greater than T_P used as the foreground for landslide remote sensing image segmentation (target object, i.e., landslide), and a value less than T_P used as the background clutter for segmentation. Assuming that in Monte Carlo iterative calculation, a pixel is identified as a target foreground above this probability threshold, then this pixel is identified as a shallow landslide mass in the final result, achieving remote sensing recognition of shallow landslide mass.

3 Results and discussions

3.1 Experimental environment and preparation

3.1.1 Experimental environment settings

The above data and DEM model require the construction of an experimental platform environment before they can be applied.

Set the experimental environment as follows: Hardware environment: Intel Core Ultra 9 285K processor, NVIDIA GeForce GTX1070 graphics card, 10 TB Seagate ST10000NM017B mechanical hard drive, 260G-SSD solid state drive.

Software environment used: Windows 11 operating system, Python programming language, MATLAB with SIMULINK simulation platform, TensorFlow model training and learning framework. Based on the above experimental environment,

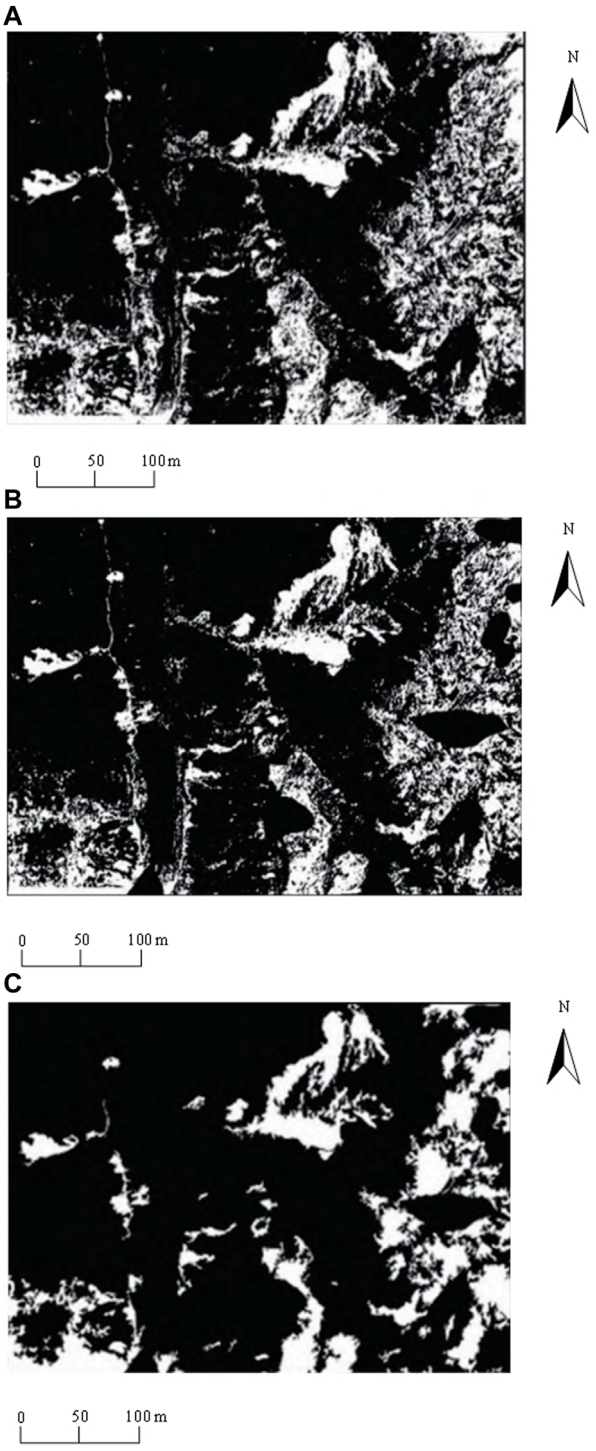

FIGURE 7
(A) Proposed method **(B)** High-resolution sensing image recognition method based on DETR **(C)** Methods based on image recognition technology and computer vision technology.

input the DEM model and data into the Revit2020 database for experimental testing.

3.1.2 Selection of local feature threshold

In order to verify the effectiveness of the shallow landslide remote sensing identification method based on the improved Otsu algorithm and multi-feature threshold proposed in this paper, the local feature threshold is first selected. When smoothing remote sensing images, a 64 × 64 pixel local window was set, and 100 local window images of landslide areas and surface types affected by geological disasters were selected for analysis. An appropriate threshold can be determined by analyzing the distribution of these images on two indicators: grayscale mean entropy and grayscale mean standard deviation. The result is shown in Figure 6. When smoothing remote sensing images, a 64 × 64 pixel local window was set, and 100 local window images of landslide areas and surface types affected by geological disasters were selected for analysis.

(a) Comparison of local window entropy and grayscale mean
(b) Comparison of local window standard deviation and grayscale mean

Figure 6 shows that the one-dimensional entropy, grayscale mean, and standard deviation values of normal ground types in non-landslide areas are lower. In contrast, the local characteristics of ground types in landslide areas exhibit higher numerical distributions. Based on the observation of Figure 6, the following thresholds can be set: the threshold for one-dimensional entropy is 4.2, the threshold for grayscale mean is 50, and the threshold for grayscale standard deviation is 20. When the eigenvalues of a local window are all less than or equal to these three thresholds, the window is classified as a normal ground type. If these conditions are not met, it is identified as a landslide type.

3.2 Analysis of identification comparison experiment results

To further verify the application effect of the shallow landslide remote sensing recognition method based on the improved Otsu algorithm and multi-feature threshold proposed in this paper, the high-resolution remote sensing image landslide recognition method based on DETR proposed in reference (Du et al., 2023) and the landslide recognition method based on image recognition technology and computer vision technology proposed in reference (Xin et al., 2023) were compared and tested together with the method proposed in this study. The binary segmentation effect of remote sensing images and the accuracy of landslide recognition will be used as experimental indicators to verify the effectiveness of different methods.

3.2.1 Binary segmentation effect

In this study, binary segmentation was performed on the target object (landslide) and background in remote sensing images. Therefore, the binary segmentation effect of different methods on remote sensing images in complex lighting environments with environmental noise interference is shown in Figure 7.

(a) Proposed method
(b) High resolution remote sensing image recognition method based on DETR
(c) Methods based on image recognition technology and computer vision technology

Figure 7 shows that although all three methods can segment the target object from the background, there is still a significant

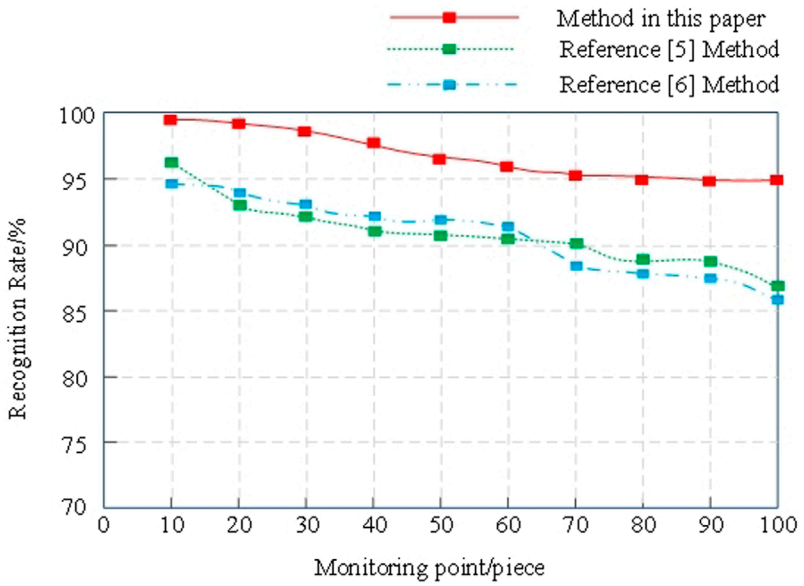

FIGURE 8
Identification rates of shallow landslide bodies using different methods.

gap in the binary segmentation effect of different methods in terms of details. Among them, the high-resolution remote sensing image landslide body recognition method based on DETR can effectively segment ordinary ground and landslide bodies. However, some areas containing vegetation have missing details, which may reduce the accuracy of shallow landslide body recognition. After binary segmentation of remote sensing images based on image recognition technology and computer vision recognition methods, some areas have high noise, blurriness, and low edge features, making it difficult to accurately segment the target object and background, which is not conducive to shallow landslide recognition. In contrast, the shallow landslide remote sensing recognition method based on the improved Otsu algorithm and multi-feature threshold proposed in this article can clearly segment the target object and background in complex lighting environments after binary segmentation of remote sensing images, with clear edges and good binary segmentation effect, which can effectively improve the accuracy of shallow landslide remote sensing recognition.

3.2.2 Accuracy of landslide identification

The accuracy of landslide identification refers to the ability to correctly identify landslide bodies (including their location, shape, size, and other information) after processing remote sensing images through specific methods. The recognition rate is a key indicator for measuring the effectiveness of landslide identification methods, which is the ratio of the number of correctly identified landslide bodies to the actual number of landslide bodies. The higher the recognition rate, the stronger the recognition ability of the method and the better the actual application effect. Arrange 150 monitoring points in the research area to monitor landslide displacement, randomly select 100 monitoring points for experimental testing, and verify the recognition rate of different methods on shallow landslide bodies in the research area. The comparison results of identification rates of shallow landslide bodies in the study area using different methods are shown in Figure 8.

Figure 8 shows that as the number of monitoring points increases, the identification rate of shallow landslide bodies using different methods shows a decreasing trend. Among them, the recognition rate of landslide bodies based on the DETR high-resolution remote sensing image recognition method decreased from 96% to 87%, with a decrease of 9 percentage points; The recognition rate based on image recognition technology and computer vision technology has decreased from 95% to 86%, a decrease of 9 percentage points. The shallow landslide remote sensing recognition method based on the improved Otsu algorithm and multi-feature threshold proposed in this article has reduced the recognition rate of shallow landslides in the study area from 99% to 95%, with a decrease of only 4 percentage points and a recognition rate of not less than 95%. This indicates that the method proposed in this article is more accurate in identifying shallow landslides in the study area and has good application effects.

4 Conclusion

This article proposes a shallow landslide remote sensing identification method based on the improved Otsu algorithm and multi-feature threshold. By conducting detailed analysis and processing of remote sensing images, the traditional Otsu algorithm has been optimized, and a multi-feature threshold strategy has been introduced to improve the accuracy and reliability of landslide identification. The experimental results show that this method can effectively distinguish landslide bodies from complex backgrounds in complex remote sensing images, accurately identify shallow landslide bodies, and provide strong technical support for early warning and prevention of geological disasters. With the continuous

advancement of remote sensing technology and the increasing richness of data sources, there is still room for further optimization of research methods, such as combining higher-resolution image data or introducing machine learning algorithms to improve recognition performance. Future research will focus on these directions to achieve higher recognition accuracy and provide more comprehensive and in-depth solutions for monitoring and managing landslide disasters.

Data availability statement

The original contributions presented in the study are included in the article/supplementary material, further inquiries can be directed to the corresponding authors.

Author contributions

JR: Conceptualization, Project administration, Resources, Writing–original draft. JW: Data curation, Formal Analysis, Funding acquisition, Investigation, Writing–original draft, Writing–review and editing. RC: Conceptualization, Writing–original draft. HL: Supervision, Writing–original draft. DX: Formal Analysis, Investigation, Writing–original draft. LY: Validation, Visualization, Writing–review and editing. JS: Conceptualization, Writing–original draft.

Funding

The author(s) declare that no financial support was received for the research, authorship, and/or publication of this article.

Acknowledgments

We thank all the authors and reviewers who were involved in this Research Topic and greatly contributed to the quality and success of the work presented here.

Conflict of interest

Authors JR, JW, RC, HL, DX, LY, and JS were employed by Sichuan Leshan Geological Engineering Survey Institute Group Co., Ltd.

Publisher's note

References

Amarasinghe, M. P., Kulathilaka, S. A. S., Robert, D. J., Zhou, A., and Jayathissa, H. A. G. (2024). Risk assessment and management of rainfall-induced landslides in tropical regions: a review. *Nat. Hazards* 120 (3), 2179–2231. doi:10.1007/s11069-023-06277-3

Deng, Z., Huang, H., Li, Q., Zhou, H., Zhang, R., Liu, Q., et al. (2024). Identification of soil landslides at the head of the Three Gorges Reservoir based on swin transformer target panoramic segmentation. *Water Resour. Hydropower Eng.* 55, 176–185. doi:10.13928/j.cnki.wrahe.2024.04.016

Du, Y., Huang, L., Zhao, Z., and Li, G. (2023). Landslide body identification and detection of high-resolution remote sensing image based on DETR. *Bull. Surv. Mapp.* (05), 16–20. doi:10.13474/j.cnki.11-2246.2023.0129

He, M., Liu, D., Zhang, M., and Li, G. (2023). A plateau mountain disaster detection model by integrating YOLOX and ASFF. *J. Disaster Prev. Mitig. Eng.* 43 (06), 1215–1223. doi:10.13409/j.cnki.jdpme.20230105002

He, N., Gao, X. H., Zhong, W., Xu, L. J., and Gurkalo, F. (2024a). A method for rapidly assessing landslide hazard-taking the landslide in Yongxing town, Mingshan area as an example. *Front. Earth Sci.* 12. doi:10.3389/feart.2024.1429346

He, N., Han, R. Z., Hu, G. S., Yang, Z. Q., Xu, L. J., and Gurkalo, F. (2024b). Evaluation of highway debris flow hazard based on geomorphic evolution theory coupled with material response rate. *Sci. Rep.* 14, 13533. doi:10.1038/s41598-024-64279-y

Jiang, H., Sun, X., Fang, W., Fu, L. S., Li, R., Cheein, F. A., et al. (2023). Thin wire segmentation and reconstruction based on a novel image overlap-partitioning and stitching algorithm in apple fruiting wall architecture for robotic picking[J].*Comput. Electron. Agric.*, 2023:209:ARTN 107840.1-107840.13.

Jiang, W., Zhang, C., Xu, B., Luo, C., Zhou, H., and Zhou, K. (2023). AED-Net:Semantic segmentation model for landslide recognition from remote sensing images. *J. Geo-information Sci.* 25 (10), 2012–2025.

König, T., Kux, H. J., and Corsi, A. C. (2022). Advanced models applied for the elaboration of landslide-prone maps, a review. *Int. J. Geosciences* 13, 174–198. doi:10.4236/ijg.2022.133010

Kusunose, T., Susaki, J., Fujiwara, Y., and Hisada, H. (2022) "PSInSAR analysis for detecting signs of landslide along expressways," in *IGARSS 2022-2022 IEEE international geoscience and remote sensing symposium*. IEEE, 2927–2930.

Li, X. S., Li, Q. L., Anisetti, M., Jeon, G., and Gao, M. L. (2023). A structure and texture revealing retinex model for low-light image enhancement. *Multimedia Tools Appl.* 83, 2323–2347. doi:10.1007/s11042-023-15242-y

Liang, X., and Sun, R. (2023). Research on new algorithm for remote sensing image noise point cloud monitoring based on full convolution network. *Comput. Simul.* 40, 205–209+219.

Lin, D., Hu, S., Wu, W. W., and Wu, G. (2023). Few-shot RF fingerprinting recognition for secure satellite remote sensing and image processing. *Sci. China-Information Sci.* 66, 189304. doi:10.1007/s11432-022-3672-7

Liu, Y., Qiu, H. J., Kamp, U., Wang, N. L., Wang, J. D., Huang, C., et al. (2024). Higher temperature sensitivity of retrogressive thaw slump activity in the Arctic compared to the Third Pole. *Sci. Total Environ.* 914, 170007. doi:10.1016/j.scitotenv.2024.170007

Neogi, S., Aich, G., Dey, A., Maitra, S., Bandyopadhyay, O., and Ghosh, K. (2024). Otsu-BRSG: an effective algorithm for river bank line detection and monitoring in the challenging terrains of kaziranga national park. *J. Indian Soc. Remote Sens.* 52, 1–20. doi:10.1007/s12524-024-01843-z

Niu, C., Gao, O., Liu, W., Lai, T., Zhang, H., and Huang, Y. (2023). Research progress of landslide detection in optical remote sensing images. *Spacecr. Recovery and Remote Sens.* 44 (03), 133–144.

Panigrahi, S. K., and Gupta, S. (2022). Phase-preserved curvelet thresholding for image denoising. *J. Institution Eng. (India) Ser. B* 103, 1719–1731. doi:10.1007/s40031-022-00780-0

Peters, S., Liu, J. X., Keppel, G., Wendleder, A., and Xu, P. L. (2024). Detecting coseismic landslides in GEE using machine learning algorithms on combined optical and radar imagery. *Remote Sens.* 16, 1722. doi:10.3390/rs16101722

Qiu, H. J., Su, L. L., Tang, B. Z., Yang, D. D., Ullah, M., Zhu, Y. R., et al. (2024). The effect of location and geometric properties of landslides caused by rainstorms and earthquakes. *Earth Surf. Process. Landforms* 49, 2067–2079. doi:10.1002/esp.5816

Rajan, K. C., Sharma, K., Dahal, B. K., Aryal, M., and Subedi, M. (2024). Study of the spatial distribution and the temporal trend of landslide disasters that occurred in the Nepal Himalayas from 2011 to 2020. *Environ. Earth Sci.* 83, 42. doi:10.1007/s12665-023-11347-7

Senogles, A., Olsen, M. J., and Leshchinsky, B. (2023). LADI: landslide displacement interpolation through a spatial-temporal Kalman filter. *Comput. and Geosciences* 180, 105451. doi:10.1016/j.cageo.2023.105451

Shen, C., Wenhao, L. I., Qisen, X. U., Bin, H. U., Bo, J., Haibin, C., et al. (2023). Interactivemedical image segmentation with self-adaptive confidence calibration. *Front. Inf. Technol. and Electron. Eng.* 24 (9), 1332–1348. doi:10.1631/fitee.2200299

Su, X., Zhang, Y., Meng, X., Ur, R. M., Zainab, K., Zhao, F., et al. (2024). Potential landslides identification and development characteristics analysis in Hunza valley,along China-Pakistan Economic Corridor based on SBAS-InSAR. *Natl. Remote Sens. Bull.* 28 (04), 885–899.

Tao, M. L., Li, J. S., Chen, J. L., Liu, Y. Y., Fan, Y. F., Su, J., et al. (2022). Radio frequency interference signature detection in radar remote sensing image using semantic cognition enhancement network. *Ieee Trans. Geoscience Remote Sens.* 60, 1–14. doi:10.1109/tgrs.2022.3190288

Wang, H., Fan, S., Huang, X., Qiu, P., Yu, J., and Li, J. (2024). Research on real-time automatic landslide recognition technology based on optical image. *Spacecr. Recovery and Remote Sens.* 45 (01), 147–160.

Wei, Y. D., Qiu, H. J., Liu, Z. J., Huangfu, W. C., Zhu, Y. R., Liu, Y., et al. (2024). Refined and dynamic susceptibility assessment of landslides using InSAR and machine learning models. *Geosci. Front.* 15, 101890. doi:10.1016/j.gsf.2024.101890

Xin, W., Pu, C. Z., Liu, W., and Liu, K. (2023). Landslide surface horizontal displacement monitoring based on image recognition technology and computer vision. *Geomorphology* 431, 108691. doi:10.1016/j.geomorph.2023.108691

Yang, Z., Zhao, Q., Gan, J., Zhang, J., Chen, M., and Zhu, Y. (2024). Damage evolution characteristics of siliceous slate with varying initial water content during freeze-thaw cycles. *Sci. total Environ.* 950, 175200. doi:10.1016/j.scitotenv.2024.175200

Ye, B. F., Qiu, H. J., Tang, B. Z., Liu, Y., Liu, Z. J., Jiang, X. Y., et al. (2024). Creep deformation monitoring of landslides in a reservoir area. *Creep deformation Monit. landslides a Reserv. area. J. Hydrology* 632, 130905. doi:10.1016/j.jhydrol.2024.130905

Zheng, W., Zuo, X., Li, Y., Li, Z., Wang, Z., and Li, D. (2024). Integration of InSAR and airborne LiDAR technologies for early landslide identification and analysis. *Bull. Surv. Mapp.* (05), 1–6. doi:10.13474/j.cnki.11-2246.2024.0501

Zhu, Y. R., Qiu, H. j., Liu, Z. J., Ye, B. F., Tang, B. Z., Li, Y. J., et al. (2024). Rainfall and water level fluctuations dominated the landslide deformation at Baihetan Reservoir, China. *J. Hydrology* 642, 131871. doi:10.1016/j.jhydrol.2024.131871